3rd National Congress on Physical Sciences, 29 Sep. – 2 Oct. 2016, Sofia
Section: Atomic Physics and Plasma Physics

Theoretical and Experimental Study on Some Plasma Parameters and Thermophysical Properties of Gas Discharges Used for Excitation of Powerful Metal and Metal Halide Vapour Lasers

K.A. Temelkov, S.I. Slaveeva, Yu.I. Fedchenko

Metal Vapour Lasers Laboratory, Institute of Solid State Physics, Bulgarian Academy of Sciences, 72 Tzarigradsko Chaussee Blvd., 1784 Sofia, Bulgaria

Abstract. Powerful metal halide vapour lasers are excited with nanosecond pulsed longitudinal discharge in complex multicomponent gas mixtures. Using a new method, thermal conductivity of various multicomponent gas mixtures is obtained under gas-discharge conditions, which are optimal for laser operation on the corresponding metal atom and ion transitions. Assuming that the gas temperature varies only in the radial direction and using the calculated thermal conductivities, an analytical solution of the steady-state heat conduction equation is found for uniform and radially nonuniform power input in various laser tube constructions. Using the results obtained for time-resolved electron temperature by measurement of electrical discharge characteristics and analytically solving steady-state heat conduction equation for electrons as well, radial distribution of time-dependent electron temperature is also obtained for the discharge period.

PACS codes: 52.80.-s; 42.55.Lt

1 Introduction

One of the main and relevant problem in the physics of gaseous discharges, gas-discharge lasers, plasma technologies and plasma in general is determination of basic plasma parameters, such as gas temperature, electron temperature, electron density, etc. The characteristic constants for the heavy-particle interaction depend on the gas temperature, while the electron temperature and electron density determine the characteristic constants for electron-heavy particle collisions. For gas-discharge lasers in particular, the above mentioned plasma characteristics influence the creation of population inversion, and hence the output laser parameters. The gas temperature distribution, i.e. the thermal mode, is also important for the stability of the laser operation.

Metal and metal halide vapour lasers are very perspective for application because of the possibility to oscillate in different spectral ranges – from deep ultraviolet (DUV) to middle infrared (MIR) ones. High beam quality and narrow-linewidth are inherent for these lasers. Several perspective high-power metal halide vapour lasers, which oscillate in DUV, visible, near infrared (NIR), and MIR spectral regions were developed, studied and applied in a number of applications, such as precise microprocessing, laser-induced modification and characterization of different materials [1-5]. These lasers are excited with nanosecond pulsed longitudinal discharge (NPLD) in complex multicomponent gas mixtures. Further improvement of these lasers requires detailed theoretical and experimental study on gas-discharge plasma parameters, such as gas temperature, electron temperature, electron density, etc., which considerably influence on laser output characteristics and stability of laser operation.

Thermal conductivity of the gas mixture considerably influences the gas temperature distribution. Due to the complex character of the existing formulae for the thermal conductivity of a multicomponent gas mixture, for example, ones based on the Wassiljewa's equation and its approximations [6], a new simple method is proposed for determination of the thermal conductivities of multicomponent gas mixtures under gas-discharge conditions, which are optimal for laser operation at the corresponding metal atom and ion lines. The method is based on iterative application of the empirical method of Brokaw [6] for binary gas systems, i.e. applying several times the Brokaw's method. Assuming that the gas temperature varies only in the radial direction and using the calculated thermal conductivities, an analytical solution of the steady-state heat conduction equation is also found for uniform and nonuniform power input in various discharge tube constructions.

Assuming that the electron temperature varied only in the radial direction and using the experimental results obtained by the line-ratio method of optical emission spectroscopy [7,8] for the space-time averaged electron temperature, a simple method based on the analytical solution of the steady-state heat conduction equation for electrons was developed for uniform and radially nonuniform power input in NPLD in He, Ne and Ne-He mixtures [9]. The time-resolved measurement of electrical discharge characteristics, such as tube voltage and discharge current, permitted us to determine the time dependence of electron temperature and electron density in the discharge period of various NPLDs, exciting several metal and metal halide vapour lasers [10]. Using these experimental results, obtained for the electron temperature, and analytically solving steady-state heat conduction equation for electrons as well, time dependence of electron temperature is also obtained for different radial distances.

2 Experimental Technique

Schematic diagrams of the laser tube (LT1) for the DUV Cu^+ Ne-H_2-CuBr laser is shown in Figure 1. The basic tube of 11.8-mm inside diameter and 15-mm outside diameter is made of fused quartz. A ceramic insert, confining the active zone, with an inside diameter of 7.1 mm, an 11.2-mm outside diameter and a length of 100 cm is coaxially sleeved in the basic tube. The CuBr powder is placed in seven quartz side-arm reservoirs, which are externally heated. The reservoir and quartz tube temperatures are measured by thermocouples.

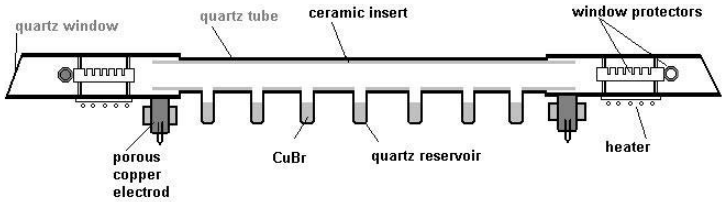

Figure 1: Laser tube construction (LT1) for DUV Cu^+ Ne–H_2-CuBr laser.

Schematic diagrams of the two used laser tubes for the MIR He-(Ne)-$SrBr_2$ laser, are shown in Figures 2(a) and 2(b), respectively. First laser tube (LT2) depicted in Figure 2(a) is without additional thermal insulation of the gas-discharge zone, while the second laser tube (LT3) given in Figure 2(b) is with additional thermal insulation of the discharge zone,

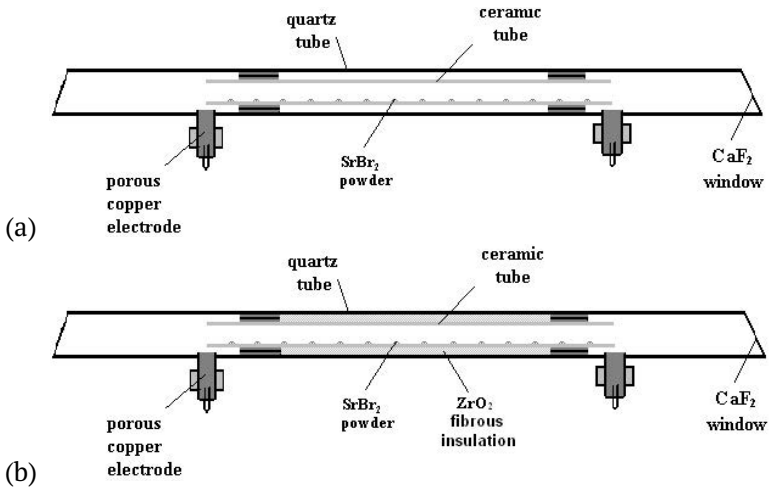

Figure 2: Laser tube constructions for MIR He–(Ne)–$SrBr_2$ laser for LT2 (a) and LT3 (b), respectively.

i.e. the zone between the ceramic insert, the basic quartz tube, and the holders of the ceramic insert is incompactly filled with ZrO_2 fibrous insulation. The basic tube with a 71.5-mm inside diameter and a 76-mm outside diameter is made of fused quartz (LT2 and LT3). A ceramic insert, confining the active zone, with a 30.5-mm inside diameter, a 38.5-mm outside diameter and a length of 98 cm is coaxially sleeved in the basic tube (LT2 and LT3). The $SrBr_2$ powder is placed inside the ceramic tube along its length. The necessary vapour pressure for laser oscillation is obtained by discharge heating; i.e. the laser operates in a self-heating regime. The laser tubes (LT2 and LT3) are wrapped by a layer of ZrO_2 fibrous insulation and its thickness depends on the power input in the discharge. The temperature at the quartz tube surface is measured by a thermocouple for both tubes.

The electrodes of the laser tubes (LT1, LT2 and LT3) are made of porous copper with a special design preventing them from contamination by CuBr, $SrBr_2$ and Br_2. The investigated NPLDs are excited by an electrical scheme with interacting circuits (IC scheme).

3 Results and Discussion

Thermal conductivities of 3-, 4-, 5- and 6-component gas mixtures are iteratively calculated. In Figure 3 the final results for thermal conductivities of several multicomponent gas mixtures are shown for gas-discharge conditions, which are optimal (DUV Cu^+ Ne-H_2-CuBr laser) or probably optimal (MIR He-(Ne)-$SrBr_2$ laser) for laser operation on the correspond-

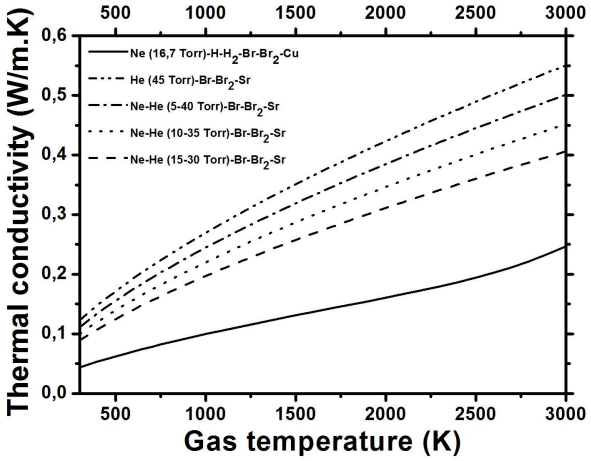

Figure 3: Thermal conductivities of various multicomponent gas mixtures as a function of gas temperature.

ing metal atom and ion transitions.

One of the important features of our tube design is that there are several zones: first, so called gas-discharge zone with radius R_1, in which the electric discharge is located, and several other zones, so called discharge-free zone within $R_i \leq r \leq R_{i+1}$ for $i \geq 1$, in which there is no power deposition. In order to obtain the gas temperature distribution, the following steady-state heat conduction equation is solved:

$$\operatorname{div}(k \operatorname{grad} T) + q_v = 0\,, \tag{1}$$

where k is the thermal conductivity, T is the temperature, which in the discharge zone is equal to the gas temperature, and q_v is the power deposited into the discharge zone per unit volume. The dependence of the thermal conductivity k has the form $k = BT^a$, where B and a are constants (within a certain temperature range), which are specific for each gas or gas mixture. Assuming that the gas temperature varies only in the radial direction, equation (1) assumes the following form:

$$\frac{1}{r}\frac{d}{dr}\left(rk\frac{dT}{dr}\right) + q_v = 0\,. \tag{2}$$

Equation (2) is solved considering the following boundary conditions:

$$\left.\frac{dT_g}{dr}\right|_{r=0}, \quad T(R_i - 0) = T(R_i + 0)\,, \quad \left.T\right|_{r=R_w} = T_w$$

and

$$k(R_i - 0)\left.\frac{dT}{dr}\right|_{R_i-0} = k(R_i + 0)\left.\frac{dT}{dr}\right|_{R_i+0} \tag{3}$$

For the case of uniform power input and taking into account (3), the equation (2) has the following analytical solution for gas temperature in the gas-discharge zone:

$$T_g(r) = \left[T_1^{a+1} + \frac{(a+1)q_V}{4B}(R_1^2 - r^2)\right]^{1/(a+1)} \tag{4}$$

and for temperature in the discharge-free zones:

$$T_i = \left[T_{i+1}^{1+a} + \frac{1+a}{2B}q_V R_1^2 \ln\frac{R_{i+1}}{R_i}\right]^{1/(1+a)} \tag{5}$$

where $i \geq 1$ and for the most outside tube wall $R_{i+1} = R_w$ and $T_{i+1} = T_w$ measured with thermocouple.

From $q_V = jE$ and $E(r) = E_0 J_0\left(\frac{2.4}{R_1}r\right)$, where $J_0\left(\frac{2.4}{R_1}r\right)$ is the Bessel function of the first kind of zero order, one can obtain $q_V =$

$Q_0 \left[J_0 \left(\frac{2.4}{R_1} r \right) \right]^2$, where the constant Q_0 remained to be obtained. In order to obtain analytical solution, a polynomial fit of the third degree is used instead of $[J_0(x)]^2$, i.e. $[J_0(x)]^2 \approx b + c.x + d.x^2 + e.x^3$, where $x = (2.4.r)/R_1$. Through fitting the following values of b, c, d and e are obtained: $b = 1.005$, $c = -0.016$, $d = -0.5702$, and $e = 0.1687$.

In this way, the following expression for q_V is obtained:

$$q_V(r) = Q_0 \left[b + c\frac{2.4}{R_1} r + d \left(\frac{2.4}{R_1} \right)^2 r^2 + e \left(\frac{2.4}{R_1} \right)^3 r^3 \right]. \tag{6}$$

Comparing the areas, bounded between the functions $q_0 = \text{const}$ and $q_V = q_V(r)$ and the variable axis r, the following expression for Q_0 is obtained:

$$Q_0 = \frac{q_0}{R_1 \left(\frac{b}{2} + \frac{c}{3} 2.4 + \frac{d}{4} 2.4^2 + \frac{e}{5} 2.4^3 \right)}. \tag{7}$$

For this case of nonuniform power deposition and taking into account (3), the solution of (2) has the following form for the discharge zone:

$$T_g = \left\{ T_1^{a+1} + \frac{(a+1)Q_0}{B} \left[\frac{b}{4}(R_1^2 - r^2) + \frac{2.4c}{9R_1}(R_1^3 - r^3) + \frac{2.4^2 d}{16R_1^2}(R_1^4 - r^4) + \frac{2.4^3 e}{25R_1^3}(R_1^5 - r^5) \right] \right\}^{\frac{1}{a+1}}, \tag{8}$$

where T_1 is calculated as in (5).

Radial temperature distribution in DUV Cu^+ Ne-H_2-CuBr laser (LT1) is presented in Figure 4 for the cases of uniform and radially nonuniform power input.

Radial temperature distribution in MIR He-(Ne)-$SrBr_2$ laser is given in Figure 5 for LT2 (1) and LT3 (2 and 3), respectively. For LT3 two cases are considered as follows: first, discharge-free zone is incompactly filled with ZrO_2 fibrous insulation (2), and second, discharge-free zone is compactly filled with ZrO_2 fibrous insulation (3), what case is not experimentally realized.

Experimental determination of radial distribution of electron temperature with measurement of relative intensity ratio of two spectral lines for NPLDs is not possible due to some insuperable obstacles encountered, namely low signal and unavoidable noise from high-power electrical pulses in the kHz range, secondary electrical pulses in the MHz region and steep rise of voltage and discharge current of TV/s and GA/s. In order to obtain electron temperature distribution in the gas-discharge

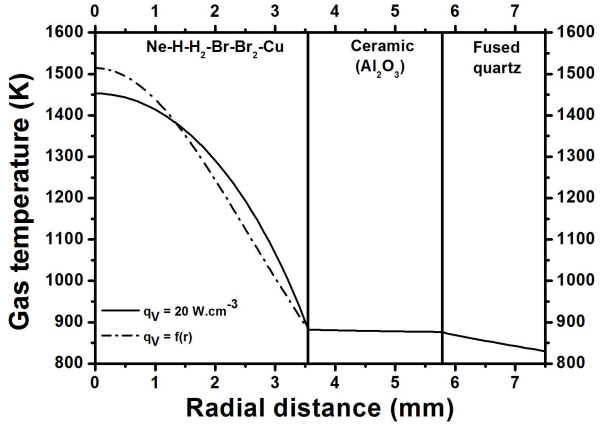

Figure 4: Radial temperature distribution in DUV Cu^+ Ne-H_2-CuBr laser.

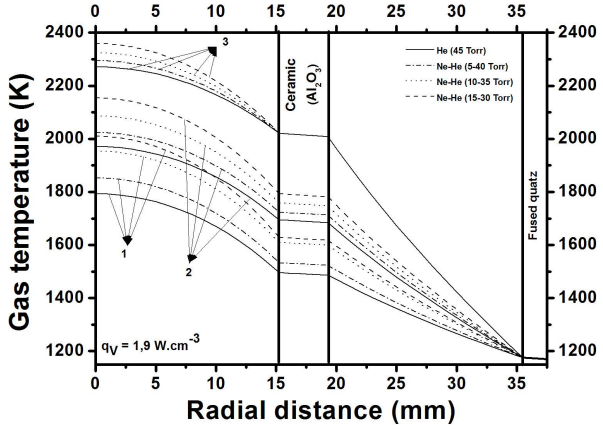

Figure 5: Radial temperature distribution in MIR He-(Ne)-$SrBr_2$ laser for LT2 (1) and LT3 (2 and 3), respectively.

zone, the following steady-state heat conduction equation:

$$\mathrm{div}\,(k_e\,\mathrm{grad}\,T_e) + \xi q_v = 0\,, \tag{9}$$

for electrons was firstly solved for uniform power input [9], where k_e is electronic thermal conductivity of the electron gas and ξq_V is electric power density deposited for electrons heating. Using Wiedemann-Franz law for electronic thermal conductivity $\dfrac{k_e}{\sigma} = cT_e$, where σ is the specific electrical conductivity, $c = \dfrac{\pi^2}{3}\left(\dfrac{k_b}{e}\right)^2$ is constant, k_b is the Boltzmann

constant, and e is the electron charge, and assuming that σ is independent of the spatial coordinates and has a value of $\bar{\sigma}$, the steady-state heat conduction equation was transformed to the given equation

$$\operatorname{div}(T_e \operatorname{grad} T_e) = -\frac{\xi q_V}{c\,\bar{\sigma}}\,. \tag{10}$$

The equation (10) is of the kind, which is typical steady-state heat conduction equation (1). It is obvious that $B = 1$, $a = 1$ and $T_w = 0$, i.e. the kinetic energy of electrons for $r = R_1$ is zero as a first approximation. Under assumption that electron temperature varies only in the radial direction equation (10) has the following solution:

$$T_e(r) = \sqrt{\frac{1}{2}\,\frac{\xi\, q_V}{c\,\bar{\sigma}}}\,\sqrt{R_1^2 - r^2}\,, \tag{11}$$

where the constant ξ remained to be obtained. The spatially averaged electron temperature in the discharge zone was found by mathematically averaging the solution (11) in the discharge zone over the radius and was made equal to the electron temperature T_e^{exp} experimentally determined by the line-ratio method of optical emission spectroscopy for the space-time averaged electron temperature, i.e. $\bar{T}_e = T_e^{exp}$. After mathematical processing the following radial electron temperature distribution was obtained

$$T_e(r) = 4\frac{T_e^{exp}}{\pi R_1}\,\sqrt{R_1^2 - r^2}\,. \tag{12}$$

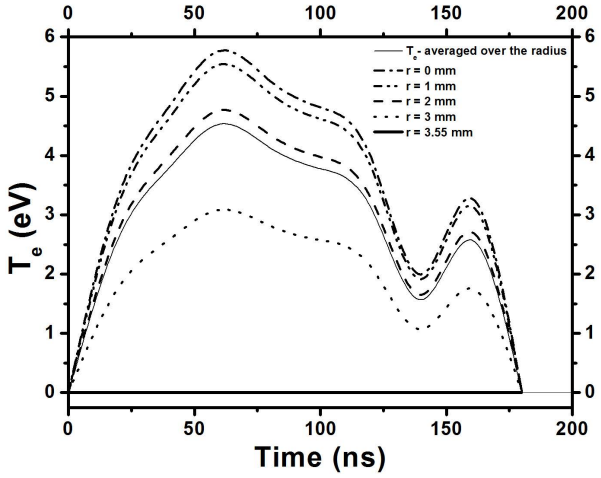

Figure 6: Time dependence of electron temperature in DUV Cu^+ Ne-H_2-CuBr laser for different radial distances.

Using the time dependence of the electron temperature T_e^{exp} determined through the time-resolved measurement of electrical discharge characteristics [10] and equation (12), radial distribution of time-dependent electron temperature is obtained. In Figure 6 temporal dependence of electron temperature is shown for different radial distances from the tube axis. The spatially averaged electron temperature [10] is also presented in Figure 6.

4 Conclusion

Utilizing of a new method, thermal conductivities of various multicomponent gas mixtures are calculated under gas-discharge conditions, which are optimal or probably optimal for laser oscillation at the corresponding metal atom and ion lines. Using the calculated thermal conductivities, radial distribution of gas temperature is also obtained in various laser tube constructions for uniform and radially nonuniform power input.

Using the results obtained for time-resolved electron temperature by measurement of electrical discharge parameters [10] and analytically solving steady-state heat conduction equation for electrons as well, radial distribution of time-dependent electron temperature is also obtained for the discharge period. Solving of the nonstationary heat conduction equation for electron gas is in progress.

References

[1] N.K. Vuchkov, K.A. Temelkov, P.V. Zahariev, N.V. Sabotinov (2001) *IEEE J. Quantum Electronics* **37** 1538-1546.

[2] N.K. Vuchkov, K.A. Temelkov, N.V. Sabotinov (2005) *IEEE J. Quantum Electronics* **41** 62-65.

[3] K.A. Temelkov, N.K. Vuchkov, B. Mao, E.P. Atanassov, L. Lyutov, N.V. Sabotinov (2009) *IEEE J. Quantum Electronics* **45** 278-281.

[4] K.A. Temelkov, N.K. Vuchkov, I. Freijo-Martin, A. Lema, L. Lyutov, N.V. Sabotinov (2009) *J. Phys. D: Appl. Phys.* **42** art. No. 115105.

[5] K.A. Temelkov, S.I. Slaveeva, V.I. Kirilov, I.K. Kostadinov, N.K. Vuchkov (2012) *Physica Scipta* **149** art. No. 014015.

[6] R.C. Reid, T.K. Sherwood (1966) *The properties of gases and liquids*, New York: McGraw-Hill Book Company, pp. 521-525.

[7] K.A. Temelkov, N.K. Vuchkov, I. Freijo-Martin, R.P. Ekov (2010) *J. Phys. D: Appl. Phys.* **43** art. No. 075206.

[8] K.A. Temelkov, S.I. Slaveeva, N.K. Vuchkov (2011) *IEEE Transactions on Plasma Science* **39** 831-835.

[9] T.P. Chernogorova, K.A. Temelkov, S.I. Slaveeva, N.K. Vuchkov (2015) in: *Proc. of SPIE* **9447** art. No. 944719.

[10] K.A. Temelkov, N.K. Vuchkov (2014) *IEEE Transactions on Plasma Science* **42** 3938-3941.